



The soluble glutathione transferase superfamily: role of Mu class in triclabendazole sulphoxide challenge in *Fasciola hepatica*

Rebekah B. Stuart¹ · Suzanne Zwaanswijk¹ · Neil D. MacKintosh¹ · Boontarikaan Witikornkul¹ · Peter M. Brophy¹ · Russell M. Morpew¹ 

Received: 27 August 2020 / Accepted: 12 January 2021 / Published online: 27 January 2021
© The Author(s) 2021

Abstract

Fasciola hepatica (liver fluke), a significant threat to food security, causes global economic loss for the livestock industry and is re-emerging as a foodborne disease of humans. In the absence of vaccines, treatment control is by anthelmintics; with only triclabendazole (TCBZ) currently effective against all stages of *F. hepatica* in livestock and humans. There is widespread resistance to TCBZ and its detoxification by flukes might contribute to the mechanism. However, there is limited phase I capacity in adult parasitic helminths with the phase II detoxification system dominated by the soluble glutathione transferase (GST) superfamily. Previous proteomic studies have demonstrated that the levels of Mu class GST from pooled *F. hepatica* parasites respond under TCBZ-sulphoxide (TCBZ-SO) challenge during in vitro culture ex-host. We have extended this finding by exploiting a sub-proteomic lead strategy to measure the change in the total soluble GST profile (GST-ome) of individual TCBZ-susceptible *F. hepatica* on TCBZ-SO-exposure in vitro culture. TCBZ-SO exposure demonstrated differential abundance of FhGST-Mu29 and FhGST-Mu26 following affinity purification using both GSH and S-hexyl GSH affinity. Furthermore, a low or weak affinity matrix interacting Mu class GST (FhGST-Mu5) has been identified and recombinantly expressed and represents a new low-affinity Mu class GST. Low-affinity GST isoforms within the GST-ome was not restricted to FhGST-Mu5 with a second likely low-affinity sigma class GST (FhGST-S2) uncovered. This study represents the most complete *Fasciola* GST-ome generated to date and has supported the potential of subproteomic analyses on individual adult flukes.

Keywords Affinity chromatography · Anthelmintic · Glutathione transferases · Proteomics

Introduction

Fasciolosis, caused by the trematode liver flukes *Fasciola hepatica* and *F. gigantica*, is a foodborne zoonotic affecting grazing animals and humans worldwide (Andrews 1999). Liver fluke causes economic losses of over US\$3 billion worldwide per annum to livestock via a decrease in production of milk, meat and wool, susceptibility to other infections, condemnation of livers and mortality (Boray 1997). There are no commercial vaccines as yet available, with triclabendazole (TCBZ) currently the most commonly used fasciolicide due to

its activity against both adults and juvenile stage fluke (Brennan et al. 2007). TCBZ is absorbed in the rumen and passes through the blood to the liver where it is rapidly oxidised to the likely main active metabolites: triclabendazole sulphoxide (TCBZ-SO) (Alvarez et al. 2005) and triclabendazole sulphone (TCBZ-SO₂) (Alvarez et al. 2009; Alvarez et al. 2005). Unfortunately, TCBZ-resistant liver flukes are wide spread, with resistance first encountered in Australia; but it is now evident in Western Europe (Brennan et al. 2007) including the UK (Thomas et al. 2000).

At present, our understanding of the mode of action and detoxification of TCBZ is fragmented and mechanisms underpinning resistance may need to be resolved in order to measure early TCBZ resistance in populations and thus preserve efficacy (Brennan et al. 2007). To this end, the glutathione transferase (GST) superfamily have been identified as the major phase II detoxification system present in all parasitic helminths. GSTs have been implicated in both drug metabolism and resistance in other groups of organisms, e.g. insects and human tumours

Section Editor: Xing-Quan ZHU

✉ Russell M. Morpew
rom@aber.ac.uk

¹ Institute of Biological, Environmental and Rural Sciences (IBERS), Aberystwyth University, Aberystwyth, Ceredigion SY23 3DA, Wales

(Hayes and Pulford 1995). Eight cytosolic GST classes have been identified and are often species-independent, including Alpha, Mu, Pi, Omega, Sigma, Theta, Phi and Zeta (Mannervik et al. 2005). In *F. hepatica*, GSTs belonging to four classes have been revealed by biochemistry and bioinformatics: Omega (ω), Mu (μ), Sigma (σ) and Zeta (ζ) (Chemale et al. 2006; Morphew et al. 2012). Chemale et al. (2010) further reported that Mu class GST levels vary, with Mu class GST-1 reduced in abundance while Mu class GST-26 increased in TCBZ-resistant and susceptible *F. hepatica* under TCBZ sulphoxide (TCBZ-SO) exposure. In addition, Scarcella et al. (2012) identified that fluke resistant to TCBZ expressed significantly higher levels of GST activity compared to susceptible flukes. Furthermore, an amino acid mutation in Mu class GST-26 has been linked to a TCBZ-resistant liver fluke strain (Fernandez et al. 2015). However, to date, there has not been a robust sub-proteomic study that compared the expression of GST isotypes in individual liver fluke under TCBZ-SO stress. Thus, we purified GSTs from the cytosol of single adult flukes using a combination of glutathione (GSH) and S-hexyl-GSH agarose, resolved GST isotypes by 2-DE and identified individual GSTs by MS/MS with the support of genomic and transcriptomic databases. As a consequence, we have identified a novel Mu, Sigma and Omega class GST-designated FhGST-Mu5, FhGST-S2 and FhGST-O2 respectively. FhGST-Mu5 has been cloned and expressed in a recombinant and active form and characterised.

Materials and methods

In vitro TCBZ culture

Individual liver flukes from natural infections were collected and exposed to TCBZ-SO as described previously (Morphew et al. 2014). In brief, live adult *F. hepatica* were collected from a local abattoir (Randall Parker Foods, Llanidloes, Wales, UK) and washed in PBS at 37 °C. Flukes were washed for 1 h with PBS replacement every 15 min. Post-washes, replicates of 10 adult, sized matched, worms were placed into fluke Dulbecco's Modified Eagle Medium (DMEM) culture media containing 15 mM HEPES, 61 mM glucose, 2.2 mM calcium acetate, 2.7 mM magnesium sulphate, 1 μ M serotonin and gentamycin (5 μ g/ml) as previously described (Morphew et al. 2011). Flukes were maintained in culture at 37 °C for 2 h (including transport to the laboratory) to establish a baseline protein expression profile. Upon completion of the initial 2-h incubation, culture media was replaced and supplemented with TCBZ-SO (LGC Standards, UK) at 50 μ g/ml (lethal dose) or 15 μ g/ml (sub-lethal dose) in DMSO (final conc. 0.1% v/v). For control samples, only DMSO was added to a final volume of 0.1% v/v. Fluke cultures were then allowed to incubate at 37 °C for a 6-h time period after which the media

was refreshed, with DMSO and TCBZ-SO as required. Fluke cultures were incubated at 37 °C for a further 6 h. A final refreshment of culture media was conducted and fluke cultures incubated for an additional 12 h at 37 °C. Upon completion of the culture, flukes were removed from the media and snap frozen individually in liquid N₂. All samples were stored at – 80 °C until required.

GST assay and purification

Individual adult *F. hepatica* were homogenised in an all-glass homogeniser on ice using 2 ml of lysis buffer containing 20 mM potassium phosphate pH 7.4, 0.1% v/v Triton-X 100 and EDTA-free protease inhibitors (Roche, Complete-Mini, EDTA-free). Samples were centrifuged at 100,000 \times g for 45 min at 4 °C to obtain the supernatant, the cytosolic fraction. Protein levels were quantified by the method of Bradford (1976). GST enzymatic specific activity was determined according to the conditions outlined by Habig et al. (1974) described previously (LaCourse et al. 2012) and stored at – 80 °C until needed. Briefly, GST activity was measured using 1 mM of the model substrate 1-chloro-2,4-dinitrobenzene (CDNB) and 1 mM reduced GSH in 20 mM potassium phosphate pH 6.5 and 25 °C. Activity was monitored at 340 nm over a period of 3 min. Specific activity data was log₁₀ transformed prior to statistical comparison carried out by a two-way ANOVA.

Cytosolic proteins were applied to a GSH-agarose (Sigma-Aldrich) or an S-hexyl-GSH-agarose (Sigma-Aldrich) affinity matrix and purified at 4 °C according to the manufacturer's instructions and as described previously (Morphew et al. 2012). Eluted proteins were concentrated using 10-kDa molecular weight cutoff filters (Amicon Ultra, Millipore) and washed with ddH₂O. All samples were quantified again by the method of Bradford (Sigma-Aldrich).

Protein preparation and 2-DE

IPG strips (7 cm, linear pH 3–10) were rehydrated with 100 μ l of buffer (containing 8 M Urea, 2% w/v CHAPS, 33 mM DTT, 0.5% ampholytes pH range 3–10) plus 25 μ l of sample protein and ddH₂O to load 20 μ g of GSH or Hexyl-GSH affinity bound proteins. Samples were in-gel rehydrated for 16 h and isoelectrically focused on 7 cm pH 3–10 IPG strips to 10,000 Vh on a Protean® IEF Cell (BioRad). After focusing, strips were then equilibrated for 15 min in reducing equilibration buffer (30% v/v glycerol, 6 M urea, 1% DTT) followed by 15 min in alkylating equilibration buffer (30% v/v glycerol, 6 M urea, 4% iodoacetamide). IPG strips were run upon SDS PAGE (12.5% acrylamide) using the Protean® II 2-D Cell (BioRad). Gels were then Coomassie blue stained (Phastgel Blue R, Amersham, Biosciences), and imaged on a GS 800 calibrated densitometer (BioRad). Quantitative differences

between 2-DE protein spots were analysed using Progenesis PG220, software version 200 (Nonlinear Dynamics Ltd.), using 5 biological replicates. Spots were automatically detected on gels and manually edited. Normalisation of spots was calculated using total spot volume multiplied by the total volume (Moxon et al. 2010). All gel images were warped using manual matching before average gels (5 gels were used to make the average gels) for each treatment group were produced. Unmatched protein spots were also detected on appropriate gel comparisons. Two-fold differences between protein spots with a $p < 0.05$ were considered significant when average gels were compared.

Western blotting

Following 2-DE, resolved proteins were transferred to nitrocellulose membranes. The nitrocellulose membrane was soaked in ddH₂O for 1 min. The gel, membrane, filter paper and porous pads were equilibrated in 1× Western Blot Transfer Buffer (NuPAGE Transfer Buffer, Life Technologies) for 20 min.

Proteins were transferred at 40 V for 2 h in 1× Western blot transfer buffer (50 ml NuPage transfer Buffer, 850 ml ddH₂O, 100 ml methanol). To ensure proteins were transferred, the membrane was removed and stained with Amido black staining solution (0.1% w/v Amido black, 10% v/v Acetic Acid, 25% v/v isopropanol) for 1 min to detect the success of the transfer. The membrane was then washed with ddH₂O. The membrane was then placed in Amido black de-stain (25% v/v isopropanol and 10% v/v acetic acid) for 30 min. The membrane was imaged using the GS-800 calibrated densitometer (BioRad). Amido black stain was removed with several washes of Tris-buffered saline, 1% v/v Tween 20 (TTBS).

The nitrocellulose membrane was blocked in blocking buffer (TTBS + 5% milk powder) overnight. The membrane was then washed with TTBS and then incubated with the primary antibody for 1–2 h. A 1:5,000 dilution and a 1:30,000 antibody dilution in blocking buffer was used for anti-Mu and anti-Sigma GST respectively. After incubation with the primary antibody, the membrane was washed in TBS for 10 min. The membrane was washed twice more before incubating with the secondary antibody (anti-goat IgG raised in rabbits for the Mu and anti-rabbit IgG raised in goats for the Sigma) for 1–2 h at a 1:30000 dilution in blocking buffer. The membrane was then washed 3 times in Tris-buffered saline (TBS). Interacting spots or bands were detected using the 5-bromo-4-chloro-3-indolyl phosphate (BCIP) in conjugation with nitro blue tetrazolium (NBT), according to manufacturer's instructions. To develop, a 1:2 solution of BCIP:NBT in substrate buffer consisting of 0.1 M tris, 100 mM NaCl and 5 mM magnesium chloride, adjusted to pH 9.5. To cease the over development, membranes were rinsed in ddH₂O. Blots were then scanned with a GS-800

calibrated densitometer (BioRad) and were imaged using Quantity One Version 4.6 software (BioRad, UK).

Protein identification

Protein spots were manually excised from the gels and in-gel digested with trypsin according to the method of Chemale et al. (2006). Tandem mass spectrometry (MSMS) was performed according to the method described by Moxon et al. (2010). Briefly, selected peptides from peptide digests were loaded onto a gold coated nanovial (Waters, UK), and sprayed at 800–900 V at atmospheric pressure and fragmented by collision-induced dissociation using argon as the collision gas. Mass Lynx v 3.5 (Waters, UK) ProteinLynx was used to process the fragmentation spectra. Each fragmented spectrum was individually processed as follows: each spectrum was combined and smoothed twice using the SavitzkyGolay method ± 3 channels, background subtraction (polynomial order 15 and 10% below the curve). Each spectrum was exported and spectra common to each 2-DE spot were merged into a single MASCOT generic format (.mgf) file using the online peak list conversion utility available at www.proteomecommons.org (Falkner et al. 2007).

Mass spectrometry database analysis

Merged files were submitted to MASCOT MSMS ion search set to search the published *F. hepatica* genomes (Cwiklinski et al. 2015; McNulty et al. 2017). The following parameters were selected for each peptide search: enzyme set at trypsin with one missed cleavage allowed, fixed modifications set for carbamidomethylation with variable modifications considered for oxidation of methionine, monoisotopic masses with unrestricted protein masses were considered, peptide and fragment mass tolerance were set at ± 1.2 Da and 0.6 Da respectively for an ESI QUAD-TDF instrument (Moxon et al. 2010).

In silico investigation of *Fasciola* transcripts and *F. hepatica* genome

Sequences representing known GST classes were obtained from NCBI (<http://www.ncbi.nlm.nih.gov/>). A mammalian and a helminth GST sequence were selected for each GST class where available. GST sequences were used to tBLASTn the *F. hepatica* transcriptome (Young et al. 2010) and the *F. gigantica* transcriptome (Young et al. 2011) both available to search at <http://bioinfosecond.vet.unimelb.edu.au/wblast2.html>. A second *F. hepatica* transcriptome database (EBI-ENA archive ERP000012: an initial characterisation of the *F. hepatica* transcriptome using 454-FLX sequencing) was also used to search against. In silico investigation of the known GST sequences and positive transcript hit were blasted against genome sequencing project of *F. hepatica* (Cwiklinski

et al. 2015) and *F. gigantica* (Choi et al. 2020). The genome of Choi et al. (2020) was chosen over that of Pandey et al. (2020) as the data is freely accessible through NCBI GenBank and Wormbase Parasite. Transcript expression levels for individual *F. hepatica* GST isoforms were analysed from Cwiklinski et al. (2018) Each specific GST isoform was used to BLASTp the transcriptome to identify the respective expression level.

Cloning of newly identified genes

PCR amplification was carried out on an Applied Biosystems 96 Well Thermal Cycler. PCR of cDNA was performed using MyFi Taq (Bioline) following the manufacturer's instructions. Standard thermocycler conditions involved an initial denaturation at 95 °C for 2 min, followed by 25–35 cycles of denaturation (95 °C, 30 s), annealing (gradient temperature specific for each gene of interest, 30 s) and extension (72 °C, 30–90 s), before a final extension at 72 °C for 5 min and holding period at 4 °C until products removed. Primers were based on the scaffolds from the *F. hepatica* genome (FhGST-S2 For: GGGCGATACTATCTATCAACGT Rev: GTGCGACT GACTTTGAATC; FhGST-O2 For: CACACAGCTGGAAT TGA TTA Rev: TAATATTGACGGATCCAAACA). PCR products were ligated into pGEM-T-Easy, according to the manufacturer's protocol and sequenced in house. Sequences were translated using ExPasy Translate (<https://web.expasy.org/translate/>) and molecular weight and pI calculated using ExPasy Compute pI/Mw (https://web.expasy.org/compute_pi/). GST domains were predicted using Pfam (El-Gebali et al. 2019).

Protein sequence alignment and phylogenetic tree construction

All sequences were aligned using ClustalW through BioEdit Version 7.0.5.3 (10/28/05) (Hall 1999). To construct a phylogenetic tree, an alignment of all GST sequences was exported into Molecular Evolutionary Genetics Analysis (MEGA) software version X (Tamura et al. 2007). Analysis was performed using a neighbour-joining method, 1000-replicate, bootstrapped tree. The amino acid data were corrected for a gamma distribution (level set at 1.0) and with a Poisson correction.

Recombinant *Fasciola hepatica* glutathione transferase Mu class (rFhGST-Mu5) production

FhGST-Mu5 was amplified via PCR using the following primer pair: rFhGST-Mu5 forward primer, 5' **CATA TGGCTCCAGTCTTA** 3'; rFhGSTMu5 reverse primer, 5' **GCGGCCGCTTA**ACTGGGTGGTGCA 3'; and a second reverse primer containing the stop codon 5' **GCGGCCG**

ACTTAACTGGGTGGTGCA 3'. Restriction enzyme sites (in bold type and underlined) for NdeI (forward primer) and NotI (reverse primer) were included so that the entire ORF could be directly cloned into the pET23a (Novagen) vector. Recombinant proteins were produced in *Escherichia coli* BL21 (DE3) cells (Bioline) as described previously (LaCourse et al. 2012; Morphew et al. 2012).

E. coli preparations containing rFhGST-Mu5 were suspended in lysis buffer (containing 5 mM MgCl, 400 mM NaCl and 20 mM sodium phosphate pH 7.4) and were lysed through a freeze/thaw method, freezing in liquid nitrogen followed by thawing at 42 °C three times. This was followed by 3 cycles of ultrasonication; the samples were sonicated for 30 s with 30-s intervals in ice. The samples were centrifuged at 13,200×g for 20 min at 4°C, and purified by GSH affinity chromatography as described previously.

Results

Limited induction of soluble *F. hepatica* GST by TCBZ-SO

Prior to affinity chromatography, GST enzymatic specific activity was assessed to examine if overall cytosolic GST activity was induced by TCBZ-SO exposure (Table 1). In general, there was a trend to increased GST-specific activity following exposure to TCBZ-SO for treatment groups compared to controls (Online Resource 1). However, following ANOVA, no significant difference was noted between any of the treatment groups or the controls (2_{df} , $F = 1.25$, $P = 0.320$).

GST proteomic profiling of individual fluke

Two affinity matrices were used to isolate GST isoforms from individual adult *F. hepatica*. Eighteen individuals were homogenised independently and all 18 independently processed through GSH or S-Hexyl GSH agarose columns to separate *F. hepatica* GST proteins from other soluble proteins. Following purification, it was possible to compare the GST-ome from each individual *F. hepatica* exposed to TCBZ-SO, either a sub-lethal concentration (15 µg/ml) or a lethal concentration (50 µg/ml), versus those not exposed using 2-DE proteomics.

Proteomic arrays of the GSTs purified from S-hexyl GSH-agarose consistently yielded 13 protein spots (Fig. 1a), whereas those purified from GSH-agarose column yielded 11 prominent protein spots (Fig. 1b). All protein spots from both purification systems were confirmed as containing *Fasciola* GSTs using tandem mass spectrometry (Table 2; full proteomic analysis Online Resource 2). Comparison of 2-DE protein arrays was then performed to establish if there was a change in abundance of the

Table 1 GST-Specific activity assays of *F. hepatica* GST samples exposed to TCBZ-SO

Treatment	Total activity (nmol/min)	Total protein (mg)	Specific activity (nmol/min/mg)
Control	4463.44	8.55	522.04 ± 77.92
Sub-lethal	6002.92	10.52	570.62 ± 190.46
Lethal	6190.82	9.35	662.12 ± 134.63

TCBZ-SO at Control (0 µg/ml), sub-lethal (15 µg/ml) or lethal (50 µg/ml) dose. Total activity (nmol/min), total protein (mg) and specific activity (nmol/min/mg) are included

identified GSTs relating to the different treatment of TCBZ-SO (Fig. 1c–f).

When comparing the S-Hexyl GSH control array with both the S-Hexyl GSH TCBZ-SO exposed arrays (Fig. 1a, c and e), it was noted that spot 14 was present on all control arrays, thus present on the average control array. However, the presence of this protein spot varied on the TCBZ-SO treatment arrays (sub-lethal and lethal). This particular protein spot was only present on 2 sub-lethal arrays (numbered in Fig. 1c) and 1 lethal array (not visible on the representative array shown in Fig. 1e). MSMS analysis identified this spot as Mu class GST29 (THD21358).

The comparison of the arrays produced via GSH agarose affinity columns identified two protein spots of interest when the average control and average sub-lethal arrays were examined with both spots increased in abundance in sub-lethal samples: spot 5, Mu class GST 26 (1_{df} , $F = 3.89$, $P = 0.089$) and spot 7, Mu class GST 29 (1_{df} , $F = 4.83$, $P = 0.064$) both approaching statistical significance (Fig. 1b and d; Online Resource 3). No additional changes in protein abundance were observed for GSH purifications.

GST expression in the cytosol of individual fluke and affinity binding

Given the recorded potential of Mu class GSTs responding to TCBZ-SO exposure, Western blotting was used to estimate the number of Mu class GSTs present in liver fluke cytosol prior to affinity chromatography, given previous indications that some GST isoforms may fail to bind to affinity matrices (Brophy et al. 1990). Assays were undertaken on five individual adult flukes using anti-*S. mansoni* Mu class polyclonal antibodies, previously shown to recognise *F. hepatica* Mu class GSTs (Chemale et al. 2006). The anti-flatworm GST Mu class antibody recognised 8 GST subunits within the cytosolic profile (Fig. 2a). Post purification, the blot patterns display the same distinctive GST protein profiles following both GSH and S-Hexyl GSH affinity 2-DE gels (Fig. 2b, c). A distinctive and reproducible 2-DE GST profile provides evidence that 8 GST subunits are recognised by the Mu antibody post purification.

Bioinformatic characterisation of GSTs identified in *F. hepatica*

Following analysis of available transcript and genome sequences, the known 4 Mu class GSTs were identified alongside a fifth Mu class GST designated FhGST-Mu5. Following cloning and sequencing of FhGST-Mu5, multiple alignment of all Mu class GSTs of *F. hepatica* revealed the extent of identity and similarity across this class of GSTs (Fig. 3a). Amino acid sequence similarity when comparing the newly identified FhGST-Mu5 (Genbank MT613329) with the previously known *F. hepatica* Mu class GSTs identified the closest sequence similarity was with FhGST-7 at approximately 54%. It is also worth noting that GenBank entry THD26413 matches to FhGST-Mu5 with 91.9% sequence identity but is an incomplete sequence lacking the N-terminus. When transcript expression was analysed for FhGST-Mu5 based on Cwiklinski et al. (2018), the levels of transcript within the adult are significantly lower than those in alternative life cycle stages such as metacercariae and newly excysted juveniles from 1 to 24 h (Fig. 3b). Of note was the identification of a homologue of FhGST-Mu5 within *F. gigantica*. Two accession numbers (TPP60771 and TPP66459) were retrieved from genome searches albeit both representing incomplete sequences.

Further transcript and genome investigation allowed the examination of the complete GST-ome of *F. hepatica* and a more complete understanding of *F. gigantica*. In addition to FhGST-Mu5, in silico investigation revealed the identification of a second Sigma class and a second Omega class GST within *F. hepatica*. Bioinformatic characterisation of the new FhGST-S2 and FhGST-O2 was undertaken to identify the structural features and characteristics of these genes/proteins. Only a single homologue for each was identified in the original *F. hepatica* genome. For FhGST-S2, gene BN1106_s1104B000225 (Scaffold 1104) was identified yet this is now fragmented and incomplete in the most recent version of the genome (PRJEB25283) despite transcript support (Online Resource 4). In addition, a *F. gigantica* homologue of FhGST-S2 was also identified in the recent genome (TPP56382). However, unlike *F. hepatica*, the *F. gigantica* genome revealed a third potential Sigma class GST (FgGST-S3; TPP56383). For FhGST-O2, gene BN1106_s50B000678

Table 2 Putative protein identification of GST isoforms from *F. hepatica* by MSMS.

Spot	MASCOT score	Genome accession number ^a	Putative ID ^b	Total peptides	Unique peptides	GST BLAST accession number	<i>Fasciola</i> GST clade	Abundance change
1	243	490 0.8	GST	39	8	ADP09370	Mu 26/51	–
	216	D915_15048	GST	31	5	THD18760	Mu 27/47	
	209	1184 0.31	GST	26	5	P31671	Mu 28/7	
	225	1043 0.18	GST	21	5	ABI79450	S1	
	62	D915_11958	GST	16	8	TPP64849	Mu 29/1	
2	125	490 0.8	GST	26	6	ADP09370	Mu 26/51	–
	105	D915_15048	GST	25	5	THD18760	Mu 27/47	
	100	1043 0.18	GST	21	5	ABI79450	S1	
	173	D915_11958	GST	10	5	TPP64849	Mu 29/1	
	92	D915_13000	GST	9	2	THD20590	Mu 28/7	
	49	61 0.52	TTL	3	2	–	–	
3	165	490 0.8	GST	48	9	ADP09370	Mu 26/51	–
	154	490 0.5	GST	34	5	P31670	Mu 27/47	
	79	D915_13000	GST	11	2	THD20590	Mu 28/7	
4	421	490 0.8	GST	84	11	ADP09370	Mu 26/51	–
	346	1184 0.31	GST	55	7	P31671	Mu 28/7	
	345	490 0.5	GST	60	6	P31670	Mu 27/47	
	67	2285 0.12	GST	6	3	THD21358	Mu 29/1	
5	1009	490 0.8	GST	165	15	ADP09370	Mu26/51	GSH SL ↑
	769	1184 0.31	GST	114	12	P31671	Mu 28/7	
	859	490 0.5	GST	111	9	P31670	Mu 27/47	
	128	D915_11958	GST	48	12	TPP64849	Mu 29/1	
	162	D915_13524	HP	25	1	–	–	
	52	1043 0.18	GST	5	3	ABI79450	S1	
	61	61 0.52	TTL	3	2	–	–	
6	645	1184 0.31	GST	113	12	P31671	Mu 28/7	–
	597	490 0.8	GST	112	12	ADP09370	Mu 26/51	
	643	D915_15048	GST	90	9	THD18760	Mu 27/47	
	284	D915_11958	GST	55	12	TPP64849	Mu 29/1	
	54	1043 0.18	GST	13	6	ABI79450	S1	
7	868	D915_11958	GST	177	19	TPP64849	Mu 29/1	GSH SL ↑
	203	490 0.8	GST	64	11	ADP09370	Mu 26/51	
	210	1184 0.31	GST	59	10	P31671	Mu 28/7	
	192	490 0.5	GST	59	9	P31670	Mu 27/47	
	154	1043 0.18	GST	15	7	ABI79450	S1	
8	No significant hits							–
9	220	1184 0.31	GST	49	11	P31671	Mu 28/7	–
	216	D915_15048	GST	43	8	THD18760	Mu 27/47	
	189	2285 0.13	GST	35	7	THD20842	Mu 26/51	
	171	D915_11958	GST	32	11	TPP64849	Mu 29/1	
	53	1043 0.18	GST	10	5	ABI79450	S1	
10	115	D915_15048	GST	44	9	THD18760	Mu 27/47	–
	106	1184 0.31	GST	36	6	P31671	Mu 28/7	
	66	D915_12658	GST	29	6	THD20842	Mu 26/51	
11	217	1043 0.18	GST	28	7	ABI79450	S1	–
	100	490 0.8	GST	19	7	ADP09370	Mu 26/51	
	87	D915_13000	GST	8	2	THD20590	Mu 28/7	
12	302	1043 0.18	GST	34	9	ABI79450	S1	–

Table 2 (continued)

Spot	MASCOT score	Genome accession number ^a	Putative ID ^b	Total peptides	Unique peptides	GST BLAST accession number	<i>Fasciola</i> GST clade	Abundance change	
68	2285	0.13	GST	8	2	THD20842	Mu 26/51		
51	D915_13000		GST	4	1	THD20590	Mu 28/7		
13	439	490	0.8	GST	86	14	ADP09370	Mu 26/51	–
401	1184	0.31	GST	63	13	P31671	Mu 28/7		
419	490	0.5	GST	63	8	P31670	Mu 27/47		
111	1043	0.18	GST	28	10	ABI79450	S1		
130	D915_11958		GST	25	9	TPP64849	Mu 29/1		
14	98	2285	0.12	GST	12	5	THD21358	Mu 29/1	HexGSH SL↓ L↓↓

MASCOT ion scores of > 42 indicate identity or extensive homology ($p < 0.05$). An accession number from GenBank relating to the top scoring BLAST hit to determine GST isoform is also reported. Changes in abundance (\uparrow or \downarrow) are denoted for 2DE spots responding to sub-lethal or lethal (SL or L) TCBZ-SO exposure for either purification method (GSH or Hex-GSH). ^a For hits from the PRJEB25283 genome version only numbers are provided that correspond to those numbers outlined in bold in the full name; maker-scaffold10x_000_pilon-snap-gene-0.0. ^b GST: glutathione transferase; TTL: tubulin-tyrosine ligase family protein; HP: hypothetical protein

(Scaffold 50) was revealed and is now designated as maker-scaffold10x_938_pilon-snap-gene-0.52/D915_03058. This was mirrored within *F. gigantica* (TPP65079). Each gene encoded for a predicted single protein isoform.

Both the newly predicted FhGST-S2 and FhGST-O2 were cloned (Online Resource 5a) and sequenced. Confirmation of the correct class assignment was performed with multiple alignment (Online Resource 5b

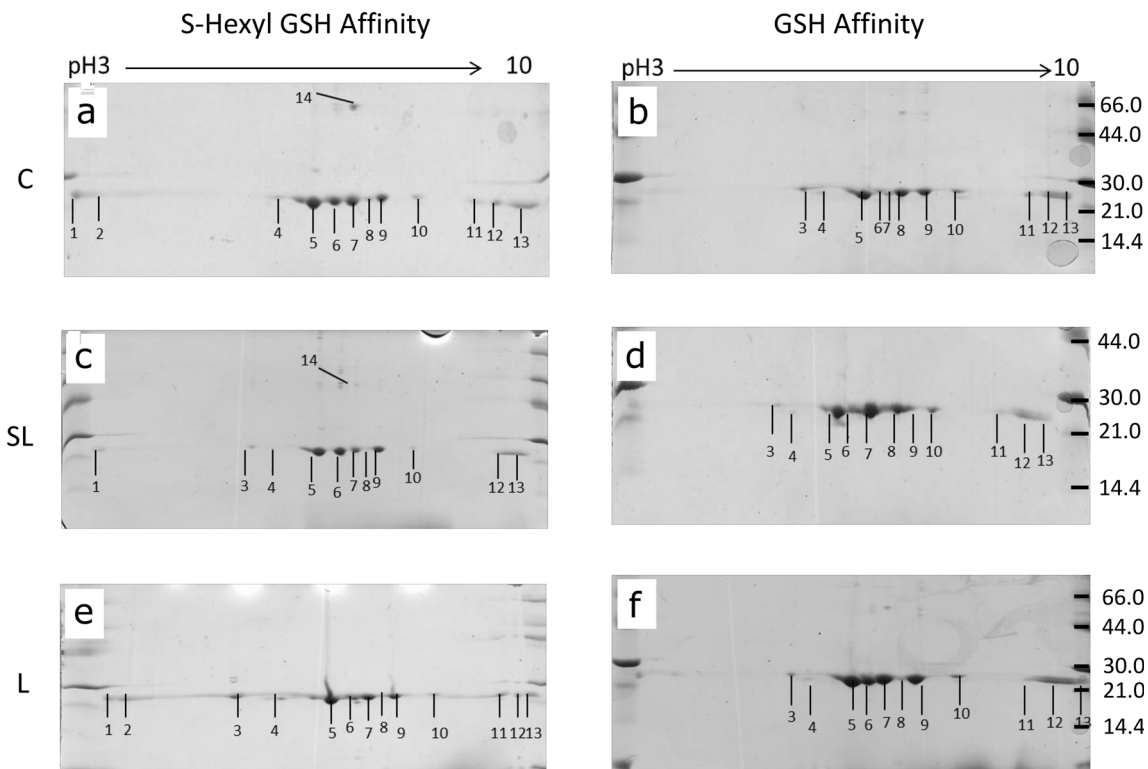


Fig. 1 Representative 2-DE arrays of GSTs purified from *F. hepatica* using S-hexyl GSH and GSH agarose columns following TCBZ-SO exposure. (a) S-hexyl GSH agarose-purified GSTs from control samples (TCBZ-SO 0 μ g/ml). (b) GSH agarose-purified GSTs from control samples (TCBZ-SO 0 μ g/ml). (c) S-hexyl GSH agarose-purified GSTs from sub-lethal samples (TCBZ-SO 15 μ g/ml). (d) GSH agarose-purified

GSTs from sub-lethal samples (TCBZ-SO 15 μ g/ml). (e) S-hexyl GSH agarose-purified GSTs from lethal samples (TCBZ-SO 50 μ g/ml). (f) GSH agarose-purified GSTs from lethal samples (TCBZ-SO 50 μ g/ml). Spot numbers relate to GST putative identifications seen in Table 2. Spot 14 shown in (a) and (c) was only present on 1 replicate of the lethal arrays and is therefore not shown in the representative array shown in (e)

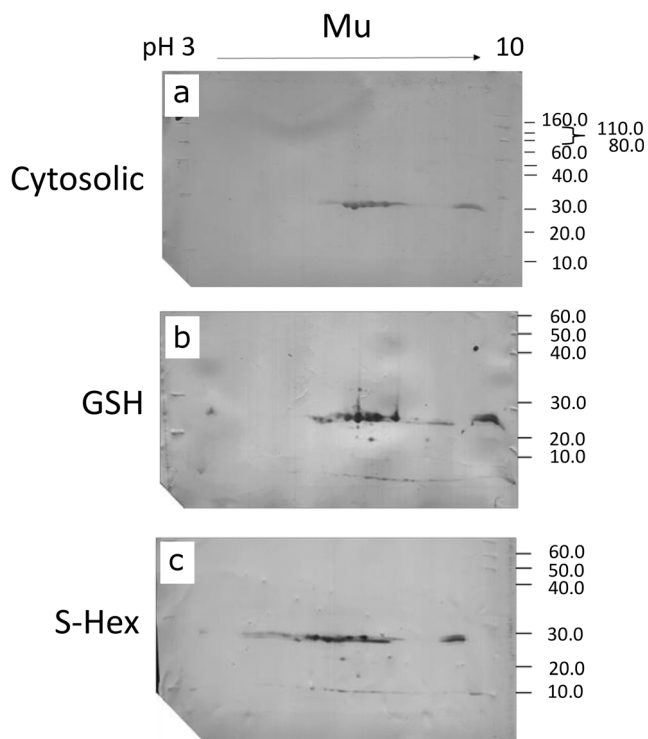


Fig. 2 Assessment of Mu class GST binding affinity through Western blotting with anti-*S. mansoni* Mu of affinity-purified GSTs in comparison to cytosolic fractions. (a) Visualisation of 100 μ g TCA precipitated cytosolic proteins of *F. hepatica* adult worms using two-dimensional gel electrophoresis (2-DE) and Western blot analysis probing for Mu class GSTs. (b, c) Visualisation of 5 μ g of GSH or S-Hexyl GSH agarose-purified GST subunits of *F. hepatica* adult worms using two-dimensional gel electrophoresis (2-DE) and Western blot analysis probing for Mu class GSTs

and 5c) and comparison of gene intron exon structure (Online Resource 6). Of note was a significant N-terminal extension of 20 amino acids in FhGST-S2 when compared to FhGST-S1. FhGST-O2 in comparison to FhGST-O1 revealed the addition of 1 amino acid to each of exons 1 and 5. Further confirmation of class assignment was supported with both FhGST-S2 and FhGST-O2 subjected to a Pfam domain analysis revealing key-predicted GST features: FhGST-S2 with a predicted C-terminal domain (Pfam GST_C_3) and FhGST-O2 with a predicted N- and C-terminal domain (Pfam GST_N_3 and GST_C_2).

Following a full phylogenetic analysis of the completed *F. hepatica* GST-ome, all of the newly identified FhGST-Mu5, FhGST-S2 and FhGST-O2, in addition to the *F. gigantica* homologues, were assigned to their respective clades (Fig. 4). Of note is the close association of FhGST-Mu5 to the Schistosoma Mu class GSTs rather than to the previously established four *Fasciola* Mu class isoforms.

Expression, purification and characterisation of rFhGST-Mu5

Full sequence length recombinant *F. hepatica* Mu class GST (rFhGST-Mu5) was expressed and purified from transformed *E. coli* cytosol following expression in BL21 (DE3) cells. Purity was assessed on SDS-PAGE gels (Fig. 3c). Interestingly, rFhGST-Mu5 was not able to be produced as a pure protein with significant levels of contaminating *E. coli* proteins remaining in the sample following GSH affinity purification. However, rFhGST-Mu5 was produced as an active protein for further studies displaying enzymatic activity towards the model GST substrate 1-chloro-2,4-dinitrobenzene (CDNB). The specific activity for the rFhGST-Mu5 preparation was confirmed at 243.27 ± 92.45 nmol/min/mg.

Discussion

The 2-DE mapping of GSTs has been shown to be a useful tool to delineate the function of individual members of this soluble protein superfamily (Chemale et al. 2006; Morphey et al. 2012), particularly as these proteins play a role in phase II detoxification (Cvilink et al. 2009). To date, research has only been completed on pooled cytosol samples from wild-type fluke and defined isolates and there has not been a robust sub-proteomic study that compared the expression of GST isotypes in individual fluke populations under TCBZ-SO challenge in culture. This study has adapted the pooled approach and, for the first time, performed analytical scale 2-DE mapping of GSTs from individual *F. hepatica* adult parasites. Thus, GSTs were purified from the cytosol of single adult flukes using either S-Hexyl-GSH or GSH agarose columns, resolved using analytical 2-DE and identified individual GSTs by MSMS with the support of liver fluke transcriptomic and genomic databases. In doing so, we can identify individual fluke responses within the GST superfamily following exposure to chemotherapeutics. Furthermore, this finding has major implications for future population and resistance monitoring studies specifically on, but not limited to, liver fluke GSTs.

In the current study, both S-Hexyl GSH agarose and GSH agarose columns were used for GST purification at the individual fluke level. Previous studies (Chemale et al. 2006; Morphey et al. 2012) have demonstrated that S-Hexyl GSH agarose columns have the ability to purify a greater range of GSTs in both *F. hepatica* and *F. gigantica* population mixes respectively, thus was a useful inclusion in the current work at the individual fluke level. Using biochemical techniques and analytical sub-proteomics identified both Sigma and Mu class GSTs purified from individual adult *F. hepatica*. It was confirmed that both S-Hexyl GSH and GSH agarose columns have the ability to purify both Mu and Sigma class GSTs,

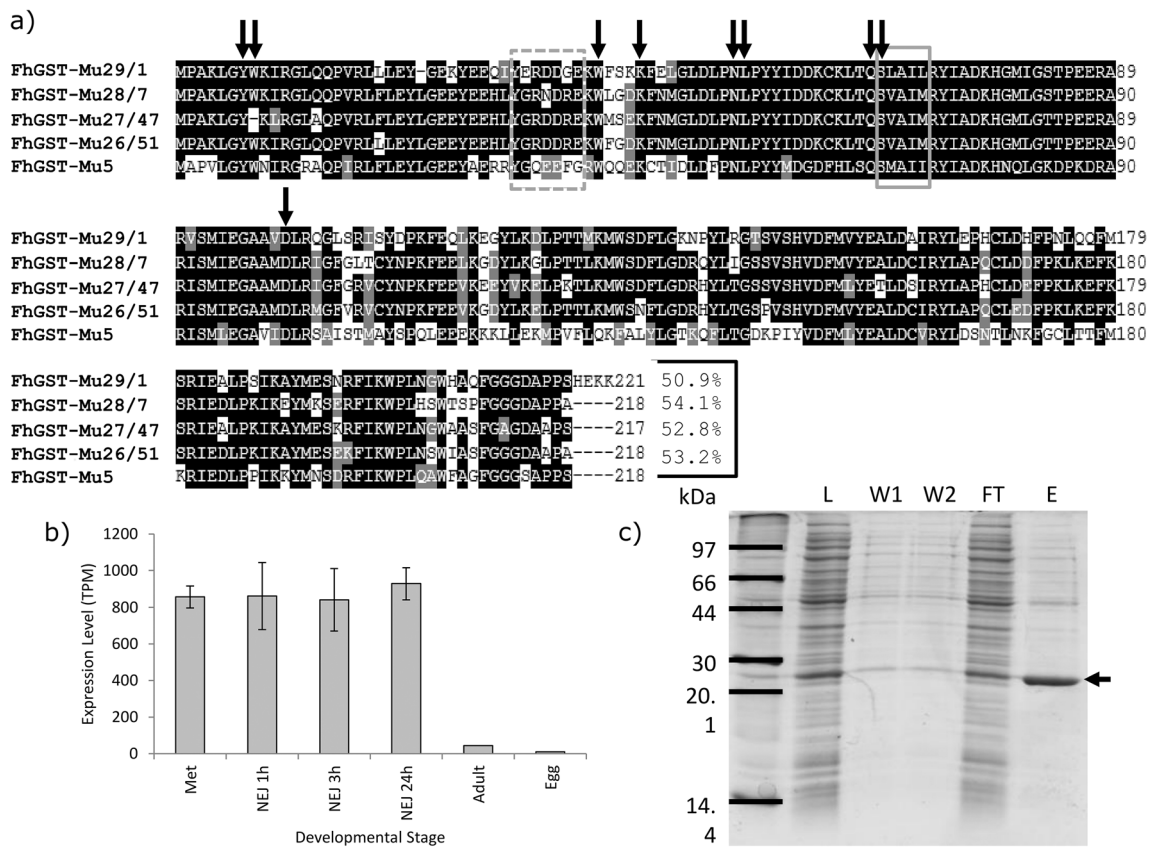


Fig. 3 Bioinformatics, expression and purification of recombinant rFhGST-Mu5. **a** Multiple sequence alignment of the 4 established *F. hepatica* Mu class GSTs and the newly identified FhGST-Mu5. No other Mu class GSTs were identified within the genome of *F. hepatica*. A putative SNAIL/TRAIL motif and their synonymous sequences in parasites are in the solid-line grey box. FhGST-Mu5 demonstrates 3 out of the 5 residues match with this motif with a fourth a highly conserved switch of the leucine residue to an isoleucine. The residues forming the μ -loop are in dotted-line grey box. Arrowed are predicted GSH-binding sites. Amino acid sequence identity of FhGST-Mu5 with the four previously known Mu class GSTs is provided at the end of the alignment. Accession

numbers for each Mu class GST used: FhGST-Mu29/1 (P56598), FhGST-Mu28/7 (P31671), FhGST-Mu27/47 (P31670) and FhGST-Mu26/51 (P30112). **b** Transcript expression levels for FhGST-Mu5 were analysed from Cwiklinski et al. (2018). **c** SDS-PAGE gel of the expression and purification of rFhGST-Mu5. L: *E. coli* total cytosolic protein lysate, 10 μ g. W1 and W2: column washes removing non-binding proteins, 10 μ l. FT: flow through proteins collected after passing through a GSH-agarose column, 10 μ g. E: eluted GSH affinity-purified recombinant rFhGST-Mu5 protein, 2 μ g. Arrowed is the band representing rFhGST-Mu5

but with GSH columns purifying the Sigma class to a much lesser extent expressing a preference to purify Mu class GSTs as observed for pooled samples (Chemale et al. 2006).

The overall GST-ome profile, via GST activity and 2-DE arrays, demonstrated a general trend of response to TCBZ-SO exposure. Following exposure, GST-specific activity increased with increasing TCBZ-SO concentration. In addition, the only changes noted in both S-Hexyl GSH and GSH agarose purifications were recorded abundance changes associated with Mu class GSTs, specifically FhGST-Mu29 and FhGST-Mu26. Therefore, from activity data and proteomic profiling, it is likely that, of the two GST classes identified, Mu class GSTs are likely highly important for xenobiotic detoxification with Sigma class GSTs acting as secondary xenobiotic sequesters with a primary role as a house-keeping enzyme and as, more importantly, an immunomodulatory (LaCourse et al. 2012). This finding of Mu class GST-TCBZ-SO detoxification

supports the work of Chemale et al. (2010) examining the TCBZ-SO response of TCBZ-resistant and TCBZ-susceptible isolates. In this case, both FhGST-Mu29 and FhGST-Mu26 responded to TCBZ-SO exposure, in agreement with the current study. We identified changes in response to TCBZ-SO exposure linked to dimer and monomer formation of FhGST-Mu29 and differential purification of both using the two purification methods. S-hexyl GSH purification was more efficient at purifying FhGST-Mu29 dimers compared to GSH agarose purification. On exposure to TCBZ-SO, a reduction in FhGST-Mu29 dimers was observed with a corresponding increase in FhGST-Mu29 monomers purified through GSH agarose. The novel dimer-monomer GST conformational switch might reflect a new liver fluke mechanism in response to TCBZ-SO challenge. GSTs normally function as dimers but active monomeric GSTs have been previously identified in *F. hepatica* (Brophy et al. 1990).

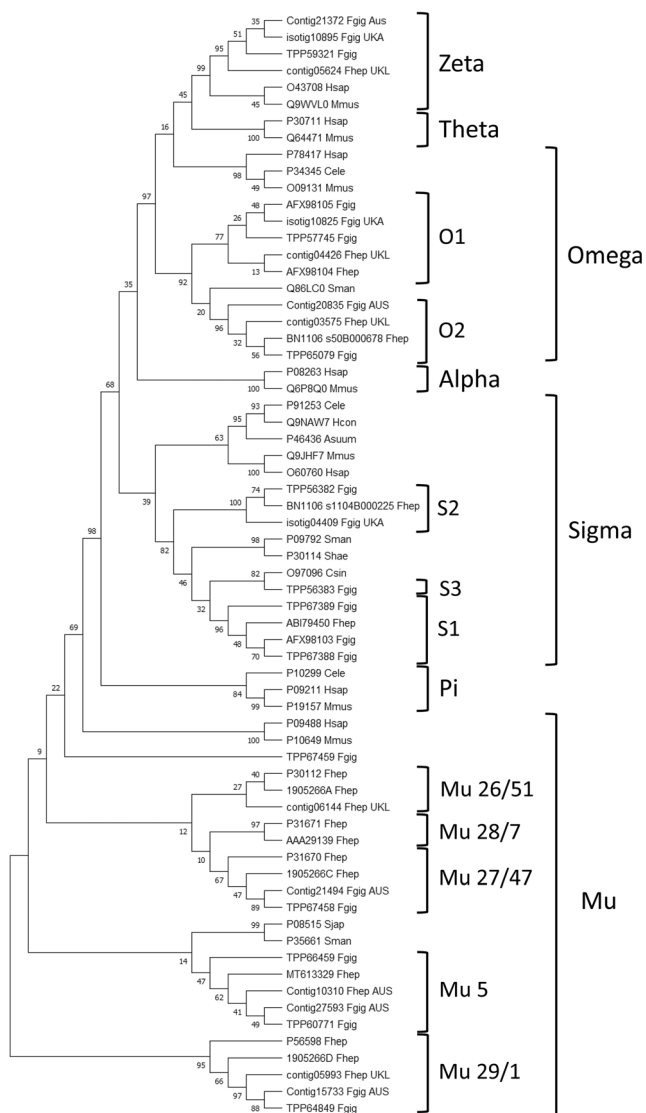


Fig. 4 Phylogenetic analysis of the soluble cytosolic GST superfamily. All reported accession numbers are from GenBank. Where sequences were identified *in silico*, only contig numbers are reported. Those from *F. gigantica* were taken from the study of Choi et al. (2020), Young et al. (2011) and transcripts produced by Aberystwyth University. Those from *F. hepatica* were taken from the study of Young et al. (2010) and transcripts produced by the University of Liverpool (EBI-ENA archive ERP000012: an initial characterisation of the *F. hepatica* transcriptome using 454-FLX sequencing)

In *F. hepatica*, there are four recognised isoforms of Mu class GSTs, i.e. FhGST-Mu26, 27, 28 and 29 (alternatively called FhGST-Mu51, 47, 7 and 1), with a fifth identified only through bioinformatics previously (Morphew et al. 2012), and now cloned and expressed in the current work. Alongside the identification of FhGST-S1, four of the five Mu class GST isoforms were identified in the samples examined in the current study under TCBZ-SO stress. In previous proteomic studies, the same four classes have also been identified. However, the functional significance of multiple Mu GSTs is as yet unknown. Multiple Mu class isoforms might relate to their role in the protection of

the parasite from various classes of xenobiotics derived from the host bile environment (Brophy et al. 2012). Specifically, the current work supports a role for FhGST-Mu29 in TCBZ-SO response via conformational changes as identified by evidence of altered in dimer/monomer ratios. Of interest, based on transcriptome evidence of Cwiklinski et al. (2018), FhGST-Mu29 is naturally the highest expressed Mu class GST in adult fluke. In addition, FhGST-Mu26 ranks third in all Mu class GST expression (FhGST-Mu29 > Mu27 > Mu26 > Mu5 > Mu28). Therefore, it is likely that these primary expressed GSTs are important in binding xenobiotics with structures such as such as TCBZ-SO.

In many cases, peptides belonging to different GSTs were identified in a single protein spot providing the identification of multiple GST isoforms. As reported by Chemale et al. (2006), this may result from spot overlapping in the 2-DE gels, as proteins may have a similar *pI*, potential modifications and co-migration. Of note is the failure to identify the fifth Mu class GST, FhGST-Mu5, despite overlapping GST isoforms identified in multiple spots. Given the sequence similarity of 54% for FhGST-Mu5 compared to FhGST-7, the failure to identify FhGST-Mu5 is unlikely to be from mis-assigning sequenced peptides to alternative Mu class GSTs and likely represents low expression as evidenced from transcriptomics (Cwiklinski et al. 2018) or, given the poor affinity purification of FhGST-Mu5, non-binding to affinity columns.

In an attempt to assess if FhGST-Mu5 was not identified in affinity-purified samples as a result of non-binding, *F. hepatica* cytosolic material was probed with anti-*S. mansoni* Mu polyclonal antibodies and compared with the profiles obtained post affinity purification. Given that the same repertoire of protein spots following Western blotting was visualised on both cytosolic and affinity-purified fractions, in addition to FhGST-Mu5 recognition by anti-*S. mansoni* Mu (data not shown), it seems unlikely that FhGST-Mu5 was missed in the affinity proteomics study. In addition, it seems unlikely that FhGST-Mu5 was missed due to low expression in adults given the identification of FhGST-Mu28 in the current work and in previous studies (Chemale et al. 2006). Thus, the potential exists that FhGST-Mu5 is a low-affinity isoform. In support, Brophy et al. (1990) proposed that an endogenous ligand interacts with GSTs preventing GST binding to the affinity matrix generating a ‘low-affinity’ fraction. Therefore, general inhibitory binding factors are likely present in the liver fluke cytosol and may be important in flatworm GST function.

Following the successful induction and expression of FhGST-Mu5, it is clear that ‘low-affinity’ GSTs are produced within the GST-ome of *F. hepatica* yet not all GSTs fail to bind from potential inhibitory factors. GSH affinity purification of rFhGST-Mu5 resulted in low impure yields of recombinant protein and suggests that FhGST-Mu5 is a ‘low-affinity’ isoform. Previous studies have all successfully used GSH affinity chromatography for successful purification of native

and recombinant GSTs (Chemale et al. 2006; LaCourse et al. 2012; Morphey et al. 2012) yet failed to purify FhGST-Mu5. Thus, to determine if rFhGST-Mu5 is an isoform with ‘low affinity’ for GSH, the specific activity was determined with the model substrate CDNB (Habig et al. 1974). The specific activity of rFhGST-Mu5 was significantly lower than that recorded for the previously known 4 Mu class GSTs from *F. hepatica* (Kalita et al. 2017; Salvatore et al. 1995). This lower affinity may be correlated with the lower sequence homology and the more distant grouping of FhGST-Mu5 in phylogenetic modelling aligning closer to schistosome Mu class GSTs rather than the previous four *F. hepatica* Mu class. Brophy et al. (1990) demonstrated that following chromatofocusing, 95% of ‘low-affinity’ GSTs were relieved of their inhibition and thus, based on current evidence, it is likely that FhGST-Mu5 could indeed be classed as a ‘low-affinity’ Mu class GST as part of the remaining 5% of activity. Low GSH affinity most likely accounts for the previous lack of detection during affinity studies with the initial identification achieved through transcriptomic analysis (Morphey et al. 2012). Given that FhGST-Mu5 clustered with schistosome Mu class GSTs during phylogenetics, it is possible that FhGST-Mu5 and schistosome Mu class GSTs perform similar roles within these fluke species. Given FhGST-Mu5 was not purified to homogeneity using GSH affinity, as evidenced by 1D SDS PAGE, additional purification steps are required in order to biochemically confirm the role of FhGST-Mu5.

The current study represents the first 2-DE profiling of TCBZ-SO exposed *F. hepatica* GSTs. However, TCBZ-SO stress in *F. gigantica*, and the resulting GST activity, has been previously investigated. Shehab et al. (2009) examined GST activities from crude homogenates of adult and juvenile *F. gigantica* exposed to TCBZ-SO concentrations. This research indicated that a significant increase in the level of GST was present, in both adult and juvenile flukes, after exposure to TCBZ-SO (Shehab et al. 2009). Such a significant increase in response to TCBZ-SO prior to affinity purification was not noted in the current research and may reflect important differences between *F. hepatica* and *F. gigantica* GST expression. Nevertheless, the work of Shehab and colleagues further supports the role of Mu class GST in TCBZ-SO detoxification.

The release of the genome assemblies of *F. hepatica* (Cwiklinski et al. 2015; McNulty et al. 2017) has allowed for further in-depth and complete investigation of the GST-ome complement of this parasitic flatworm. This has additionally been supported with the release of a genome for *F. gigantica* (Choi et al. 2020). Two new soluble superfamily GSTs were identified in *F. hepatica*; a second Sigma (σ) class and a second Omega (ω) class, on original genes BN1106_s1104B000225 and BN1106_s50B000678 (scaffolds 1104 and 50, respectively). Both GSTs contained Pfam IDs for the respective GSTs and both sequences were successfully amplified through PCR and sequence verified. The predicted molecular weight of the sub-

units of the newly identified Sigma and Omega GSTs was shown to be 26 and 27 kDa, respectively, and this is in general agreement with known soluble GSTs that have a subunit mass of between 23 and 28 kDa with an average length of 220 amino acids (Torres-Rivera and Landa 2008). Gene structure analysing introns and exons for both the newly identified Sigma and Omega genes in comparison with the previously identified *F. hepatica* Sigma and Omega supported the confirmation of GST class assignment.

Previous research has demonstrated that model organisms (humans and mice) both encode for 2 Omega class GST genes which are widely expressed (Board 2011) reflecting expression within *F. hepatica* and now *F. gigantica*, albeit human and mice omega GSTs comprise of six exons (Board 2011) rather than 5 in *F. hepatica* omega class GSTs. Interestingly, omega class GSTs have been linked with drug resistance in human cancers (Townsend and Tew 2003) and Alzheimer’s disease (Allen et al. 2012) and thus may have some role in anthelmintic resistance or detoxification not yet discovered.

Sigma class GSTs in *F. hepatica* were also initially identified by Chemale et al. (2006). A recombinant form of *F. hepatica* Sigma class GST, FhGST-S1, has since been produced and demonstrated to have multi-functional roles, including general endogenous detoxification, and is strongly linked with prostaglandin synthesis and the modulation of dendritic cell activity (LaCourse et al. 2012). Across trematode species, the exon-intron structure of Sigma class GSTs is conserved. Recently, reports of 5 newly identified Sigma class GSTs from *Clonorchis sinensis* consist of 4 exons akin to the two *F. hepatica* genes (Bae et al. 2016). It was also noted that the final exon, exon 4, of Sigma GST genes in the gene predictions of all the trematode species investigated by Bae et al. (2016) consisted of 225 bp; this conservation of gene structure likely reflects conserved biological function. As yet, proteomic investigations have not identified FhGST-S2 from adult flukes despite their presence in adult transcriptomes. It is therefore likely that FhGST-S2 remains part of the unbound fraction of the GST-ome; a likely ‘low-affinity’ sigma class GST. Interestingly, bioinformatics has revealed a potential expansion of the Sigma class GSTs within *F. gigantica* with a third potential member identified clustering alongside a *C. sinensis* Sigma class GST. Further in-depth experimentation will be required to confirm this finding.

With a key role for GSTs in the detoxification of TCBZ demonstrated through proteomic profiling, it is now crucial to understand any involvement of GSTs in TCBZ resistance. This is of particular importance given that Scarcella et al. (2012) identified that fluke resistant to TCBZ expressed significantly higher levels of GST activity compared to susceptible flukes. The authors suggest that under TCBZ-SO exposure, there is an increased requirement for phase I detoxification of TCBZ-SO, to the less-effective TCBZ-SO₂, and thus also require increased phase II detoxification, principally from GSTs, to catalyse TCBZ intermediates. Given the recent bioinformatics

identification of a potential Cytochrome P450 (Cwiklinski et al. 2015), TCBZ-SO exposure is likely to stimulate this phase I pathway leading to an increased requirement for phase II GSTs. Therefore, profiling the specific GST isoforms will give more insight into resistance mechanisms.

Conclusions

GSTs are a multi-gene family of ubiquitous multifunctional proteins that are predicted to have major roles in detoxifying both endogenous and exogenous toxins as part of the phase II system. We have expanded the knowledge on this important protein family in the parasitic flatworm *F. hepatica*. In doing so, we have revealed 5 Mu class, 2 Sigma class (3 in *F. gigantica*), 2 Omega class and 1 Zeta class GSTs including novel ‘low-affinity’ Mu and Sigma class enzymes. In addition, it is clear that GSTs respond to TCBZ-SO exposure and the role of GSTs in TCBZ resistance awaits further investigation. Finally, the ability to incorporate individual fluke for proteomic and sub-proteomic studies has implications for potential early TCBZ resistance monitoring in liver fluke populations.

Supplementary Information The online version contains supplementary material available at <https://doi.org/10.1007/s00436-021-07055-5>.

Acknowledgements The authors are grateful to Randall Parker Foods (Wales) for providing *F. hepatica*-infected sheep livers.

Authors' contributions Peter Brophy and Russell Morphew contributed to the study conception and design. Rebekah Stuart, Suzanne Zwaanswijk, Neil MacKintosh, Boontarikaan Witikomkul and Russell Morphew contributed to material preparation, data collection and analysis. The first draft of the manuscript was written by Rebekah Stuart and all authors commented on previous versions of the manuscript. All authors read and approved the final manuscript.

Funding This work was supported by the Biotechnology and Biological Sciences Research Council through an IBERS PhD Scholarship award and through Innovate UK (Grant Number: 102108).

Data availability Full proteomics datasets are provided as an [online resource](#). All raw files associated with the proteomics are available from the corresponding author on reasonable request.

Code availability Not applicable.

Declarations

Ethics approval Not applicable

Consent to participate Not applicable

Consent for publication Not applicable

Conflict of interest The authors declare that they have no conflict of interest

Open Access This article is licensed under a Creative Commons Attribution 4.0 International License, which permits use, sharing, adaptation, distribution and reproduction in any medium or format, as long as you give appropriate credit to the original author(s) and the source, provide a link to the Creative Commons licence, and indicate if changes were made. The images or other third party material in this article are included in the article's Creative Commons licence, unless indicated otherwise in a credit line to the material. If material is not included in the article's Creative Commons licence and your intended use is not permitted by statutory regulation or exceeds the permitted use, you will need to obtain permission directly from the copyright holder. To view a copy of this licence, visit <http://creativecommons.org/licenses/by/4.0/>.

References

- Allen M, Zou FG, Chai HS, Younkin CS, Miles R, Nair AA, Crook JE, Pankratz VS, Carrasquillo MM, Rowley CN, Nguyen T, Ma L, Malphrus KG, Bisceglia G, Ortolaza AI, Palusak R, Middha S, Maharjan S, Georgescu C, Schultz D, Rakhshan F, Kolbert CP, Jen J, Sando SB, Aasly JO, Barcikowska M, Uitti RJ, Wszolek ZK, Ross OA, Petersen RC, Graff-Radford NR, Dickson DW, Younkin SG, Ertekin-Taner N (2012) Glutathione S-transferase omega genes in Alzheimer and Parkinson disease risk, age-at-diagnosis and brain gene expression: an association study with mechanistic implications. *Mol Neurodegener* 7:13. <https://doi.org/10.1186/1750-1326-7-13>
- Alvarez LI, Solana HD, Mottier ML, Virkel GL, Fairweather I, Lanusse CE (2005) Altered drug influx/efflux and enhanced metabolic activity in triclabendazole-resistant liver flukes. *Parasitology* 131:501–510. <https://doi.org/10.1017/s0031182005007997>
- Alvarez L, Moreno G, Moreno L, Ceballos L, Shaw L, Fairweather I, Lanusse C (2009) Comparative assessment of albendazole and triclabendazole ovicidal activity on *Fasciola hepatica* eggs. *Vet Parasitol* 164:211–216. <https://doi.org/10.1016/j.vetpar.2009.05.014>
- Andrews SJ (1999) The life cycle of *Fasciola hepatica*. In: Dalton JP (ed) *Fasciolosis*. C. A. B. International, Oxford, pp 1–30
- Bae YA, Kim JG, Kong Y (2016) Phylogenetic characterization of *Clonorchis sinensis* proteins homologous to the sigma-class glutathione transferase and their differential expression profiles. *Mol Biochem Parasitol* 206:46–55. <https://doi.org/10.1016/j.molbiopara.2016.01.002>
- Board PG (2011) The omega-class glutathione transferases: structure, function, and genetics. *Drug Metab Rev* 43:226–235. <https://doi.org/10.3109/03602532.2011.561353>
- Boray JC (1997) Chemotherapy of infections with fasciolidae. In: Boray JC (ed) *Immunology, pathobiology and control of Fasciolosis*. MSD AGVET, Rahway, pp 83–97
- Bradford MM (1976) Rapid and sensitive method for quantitation of microgram quantities of protein utilizing principle of protein dye binding. *Anal Biochem* 72:248–254
- Brennan GP, Fairweather I, Trudgett A, Hoey E, McCoy MCM, Meaney M, Robinson M, McFerran N, Ryan L, Lanusse C, Mottier L, Alvarez L, Solana H, Virkel G, Brophy PM (2007) Understanding triclabendazole resistance. *Exp Mol Pathol* 82:104–109. <https://doi.org/10.1016/j.yexmp.2007.01.009>
- Brophy PM, Crowley P, Barrett J (1990) Detoxification reactions of *Fasciola hepatica* cytosolic glutathione transferases. *Mol Biochem Parasitol* 39:155–162
- Brophy PM, Mackintosh N, Morphew RM (2012) Anthelmintic metabolism in parasitic helminths: proteomic insights. *Int J Parasitol* 139:1205–1217
- Chemale G, Morphew R, Moxon JV, Morassuti AL, LaCourse EJ, Barrett J, Johnston DA, Brophy PM (2006) Proteomic analysis of glutathione

- transferases from the liver fluke parasite, *Fasciola hepatica*. *Proteomics* 6:6263–6273. <https://doi.org/10.1002/pmic.200600499>
- Chemale G, Perally S, LaCourse EJ, Prescott MC, Jones LM, Ward D, Meaney M, Hoey E, Brennan GP, Fairweather I, Trudgett A, Brophy PM (2010) Comparative proteomic analysis of triclabendazole response in the liver fluke *Fasciola hepatica*. *J Proteome Res* 9:4940–4951
- Choi YJ, Fontenla S, Fischer PU, Le TH, Costabile A, Blair D, Brindley PJ, Tort JF, Cabada MM, Mitreva M (2020) Adaptive radiation of the flukes of the family *Fasciolidae* inferred from genome-wide comparisons of key species. *Mol Biol Evol* 37:84–99. <https://doi.org/10.1093/molbev/msv204>
- Cvilink V, Lamka J, Skalova L (2009) Xenobiotic metabolizing enzymes and metabolism of anthelmintics in helminths. *Drug Metab Rev* 41:8–26
- Cwiklinski K, Dalton JP, Dufresne PJ, La Course J, Williams DJL, Hodgkinson J, Paterson S (2015) The *Fasciola hepatica* genome: gene duplication and polymorphism reveals adaptation to the host environment and the capacity for rapid evolution. *Genome Biol* 16:71. <https://doi.org/10.1186/s13059-015-0632-2>
- Cwiklinski K, Jewhurst H, McVeigh P, Barbour T, Maule AG, Tort J, O'Neill SM, Robinson MW, Donnelly S, Dalton JP (2018) Infection by the helminth parasite *Fasciola hepatica* Requires Rapid Regulation of Metabolic, Virulence, and Invasive Factors to Adjust to Its Mammalian Host. *Mol Cell Proteomics* 17:792–809. <https://doi.org/10.1074/mcp.RA117.000445>
- El-Gebali S, Mistry J, Bateman A, Eddy SR, Luciani A, Potter SC, Qureshi M, Richardson LJ, Salazar GA, Smart A, Sonnhammer ELL, Hirsh L, Paladin L, Piovesan D, Tosatto SCE, Finn RD (2019) The Pfam protein families database in 2019. *Nucleic Acids Res* 47:D427–D432. <https://doi.org/10.1093/nar/gky995>
- Falkner JA, Falkner JW, Andrews PC (2007) ProteomeCommons.org IO Framework: reading and writing multiple proteomics data formats. *Bioinformatics* 23:262–263. <https://doi.org/10.1093/bioinformatics/btl573>
- Fernandez V, Estein S, Ortiz P, Luchessi P, Solana V, Solana H (2015) A single amino acid substitution in isozyme GST mu in triclabendazole resistant *Fasciola hepatica* (Sligo strain) can substantially influence the manifestation of anthelmintic resistance. *Exp Parasitol* 159:274–279. <https://doi.org/10.1016/j.exppara.2015.10.007>
- Habig WH, Pabst MJ, Jakoby WB (1974) Glutathione S-transferases: the first enzymatic step in mercapturic acid formation. *J Biol Chem* 249:7130–7139
- Hall TA (1999) BioEdit: a user-friendly biological sequence alignment editor and analysis program for Windows 95/98/NT. *Nucleic Acids Symp Ser* 41:95–98
- Hayes JD, Pulford DJ (1995) The glutathione S-Transferase supergene family: regulation of GST and the contribution of the isoenzymes to cancer chemoprotection and drug resistance. *Crit Rev Biochem Mol Biol* 30:445–600. <https://doi.org/10.3109/10409239509083491>
- Kalita J, Shukla R, Shukla H, Gadhav K, Giri R, Tripathi T (2017) Comprehensive analysis of the catalytic and structural properties of a mu-class glutathione s-transferase from *Fasciola gigantica*. *Sci Rep* 7:17547. <https://doi.org/10.1038/s41598-017-17678-3>
- LaCourse JE, Perally S, Morphew RM, Moxon JV, Prescott MC, Dowling D, O'Neill SM, Kipar A, Hetzel U, Hoey E, Zafra R, Buffoni L, Arevalo JP, Brophy PM (2012) The sigma class glutathione transferase of the liver fluke *Fasciola hepatica*. *Plos Neglect Trop D* 6:e1666
- Mannervik B, Board PG, Hayes JD, Listowsky I, Pearson WR (2005) Nomenclature for mammalian soluble glutathione transferases. *Methods Enzymol* 401:1–8
- McNulty SN, Tort JF, Rinaldi G, Fischer K, Rosa BA, Smircich P, Fontenla S, Choi YJ, Tyagi R, Hallsworth-Pepin K, Mann VH, Kammili L, Latham PS, Dell'Oca N, Dominguez F, Carmona C, Fischer PU, Brindley PJ, Mitreva M (2017) Genomes of *Fasciola hepatica* from the Americas reveal colonization with *Neorickettsia* endobacteria related to the agents of potomac horse and human sennetsu fevers. *PLoS Genet* 13(1):e1006537. <https://doi.org/10.1371/journal.pgen.1006537>
- Morphew RM, Wright HA, LaCourse EJ, Porter J, Barrett J, Woods DJ, Brophy PM (2011) Towards delineating functions within the *Fasciola* secreted cathepsin I protease family by integrating *in vivo* based sub-proteomics and phylogenetics. *PLoS Negl Trop Dis* 5:e937. <https://doi.org/10.1371/journal.pntd.0000937>
- Morphew RM, Eccleston N, Wilkinson TJ, McGarry J, Perally S, Prescott M, Ward D, Williams D, Paterson S, Raman M, Ravikumar G, Saifullah MK, Abidi SMA, McVeigh P, Maule AG, Brophy PM, LaCourse EJ (2012) Proteomics and *in silico* approaches to extend understanding of the glutathione transferase superfamily of the tropical liver fluke *Fasciola gigantica*. *J Proteome Res* 11:5876–5889
- Morphew RM, MacKintosh N, Hart EH, Prescott M, LaCourse EJ, Brophy PM (2014) *In vitro* biomarker discovery in the parasitic flatworm *Fasciola hepatica* for monitoring chemotherapeutic treatment. *EuPA Open Proteom* 3:85–99
- Moxon JV, LaCourse EJ, Wright HA, Perally S, Prescott MC, Gillard JL, Barrett J, Hamilton JV, Brophy PM (2010) Proteomic analysis of embryonic *Fasciola hepatica*: characterization and antigenic potential of a developmentally regulated heat shock protein. *Vet Parasitol* 169:62–75. <https://doi.org/10.1016/j.vetpar.2009.12.031>
- Pandey T, Ghosh A, Todur VN, Rajendran V, Kalita P, Kalita J, Shukla R, Chetri PB, Shukla H, Sonkar A, Lyngdoh DL, Singh R, Khan H, Nongkhaw J, Das KC, Tripathi T (2020) Draft genome of the liver fluke *Fasciola gigantica*. *ACS Omega* 5:11084–11091. <https://doi.org/10.1021/acsomega.0c00980>
- Salvatore L, Wijffels G, Sexton JL, Panaccio M, Mailer S, McCauley I, Spithill TW (1995) Biochemical analysis of recombinant glutathione S-transferase of *Fasciola hepatica*. *Mol Biochem Parasitol* 69:281–288
- Scarcella S, Lamenza P, Virkel G, Solana H (2012) Expression differential of microsomal and cytosolic glutathione-S-transferases in *Fasciola hepatica* resistant to triclabendazole. *Mol Biochem Parasitol* 181:37–39. <https://doi.org/10.1016/j.molbiopara.2011.09.011>
- Shehab AY, Ebeid SM, El-Samak MY, Hussein NM (2009) Detoxifying and anti-oxidant enzymes of *Fasciola gigantica* worms under triclabendazole sulphoxide (TCBZ-SX): an *in vitro* study. *J Egypt Soc Parasitol* 39:73–83
- Tamura K, Dudley J, Nei M, Kumar S (2007) MEGA4: molecular evolutionary genetics analysis (MEGA) software version 4.0. *Mol Biol Evol* 24:1596–1599
- Thomas I, Coles GC, Duffus K (2000) Triclabendazole-resistant *Fasciola hepatica* in southwest Wales. *Vet Rec* 146:200–200
- Torres-Rivera A, Landa A (2008) Glutathione transferases from parasites: a biochemical view. *Acta Trop* 105:99–112. <https://doi.org/10.1016/j.actatropica.2007.08.005>
- Townsend DM, Tew KD (2003) The role of glutathione-S-transferase in anti-cancer drug resistance. *Oncogene* 22:7369–7375. <https://doi.org/10.1038/sj.onc.1206940>
- Young ND, Hall RS, Jex AR, Cantacessi C, Gasser RB (2010) Elucidating the transcriptome of *Fasciola hepatica* - a key to fundamental and biotechnological discoveries for a neglected parasite. *Biotechnol Adv* 28:222–231. <https://doi.org/10.1016/j.biotechadv.2009.12.003>
- Young ND, Jex AR, Cantacessi C, Hall RS, Campbell BE, Spithill TW, Tangkawattana S, Tangkawattana P, Laha T, Gasser RB (2011) A portrait of the transcriptome of the neglected trematode, *Fasciola gigantica*-biological and biotechnological implications. *PLoS Negl Trop Dis* 5:e1004. <https://doi.org/10.1371/journal.pntd.0001004>